Tunable multi-cycle terahertz pulse generation from a spintronic emitter

DOI:
10.1063/5.0176314

Document Version
Accepted author manuscript

Tunable multi-cycle terahertz pulse generation from a spintronic emitter

R. Ji,[1,2] M. T. Hibberd,[2,3] C.-H. Lin,[1,2] D. A. Walsh,[3,4] T. Thomson,[1] P. W. Nutter,[1] and D. M. Graham[2,3]

[1)]*Nano Engineering and Spintronic Technologies Group, Department of Computer Science, The University of Manchester, Oxford Road, Manchester M13 9PL, United Kingdom*

[2)]*Department of Physics and Astronomy & Photon Science Institute, The University of Manchester, Oxford Road, Manchester M13 9PL, United Kingdom*

[3)]*The Cockcroft Institute, Sci-Tech Daresbury, Keckwick Lane, Daresbury, Warrington WA4 4AD, United Kingdom*

[4)]*Accelerator Science and Technology Centre, Science and Technology Facilities Council, Sci-Tech Daresbury, Keckwick Lane, Daresbury, Warrington WA4 4AD, United Kingdom*

(*Electronic mail: Darren.Graham@manchester.ac.uk)

(Dated: 5 October 2023)

We demonstrate that a spintronic terahertz (THz) emitter can be driven by a chirped-pulse beating scheme to generate narrowband THz pulses, with continuous tuning of the frequency and linewidth by simply adjusting the laser chirp and/or the time delay between chirped pulses. As supported by model calculations, temporal shaping of the drive laser pulses can be exploited to manipulate the ultrafast demagnetization dynamics in the thin-film emitter, modulating the spin-polarized current in the ferromagnetic layer to access multi-cycle THz emission. Using a regenerative amplifier laser system with 50 fs transform-limited pulses chirped to 6 ps, we demonstrate narrowband THz generation over a frequency range from 0.4 to 2.3 THz, in addition to linewidths down to 40 GHz using 12 ps chirped pulses. Our proof-of-concept results pave the way to future narrowband THz sources with sub-GHz linewidth and center frequencies continuously tunable from 0.1 to 30 THz. Combined with the advantageous properties of spintronic THz emitters, from straightforward implementation to flexible polarization control, these sources open up opportunities for narrowband applications over the entire THz spectral range.

Underpinned by early experiments on ultrafast laser-induced ferromagnetic demagnetization[1], the development of spintronic terahertz (THz) emitters by Kampfrath *et al.*[2] has initiated rapid progress that has established these nm-scale metallic heterostructures as unique sources in the field of THz science.[3] They offer high-field (>1 MV/cm)[4], ultra-broadband (up to 30 THz)[5], gap-free emission with photo-excitation over a wide spectral range, no phase-matching or complex alignment requirements, and low-cost fabrication that is scalable to large sizes.[6] Additionally, they can provide flexible polarization control using external magnetic fields[7–9] and even field-free operation exploiting magnetic anisotropy[9]. These desirable properties have been exclusively demonstrated with broadband single-cycle THz pulses, but there is significant interest in the generation and exploitation of laser-driven narrowband THz sources, with applications across a broad range of research areas including selective excitation of resonant modes (in layered superconductors[10], quantum wells[11] and ferroelectric thin films[12]), non-linear microscopy[13] and compact particle accelerators[14].

Numerous materials combined with various optical techniques have been used to achieve narrowband THz generation. These include chirped-pulse beating schemes in photoconductive antennas[15–17], organic materials (HMQ-TMS[18], OH1[19], DSTMS[20]), inorganic non-linear crystals (ZnTe[21], $LiNbO_3$[22]) and air-plasma[23], as well as difference frequency generation in GaSe[24] and DSTMS[25], quasi-phase-matching schemes in periodically-poled GaAs[26], GaP[27], $LiNbO_3$[28–30] and Rb:KTP[31] crystals, and parametric generation schemes[32–34]. Recent alternatives include phase-matched optical rectification in a range of bulk crystals[35] and the use of an echelon in a bulk $LiNbO_3$ crystal[36].

Given the advantageous properties of spintronic THz emitters, the additional capability for narrowband emission has already begun to attract interest. Excitation of ferrimagnetic nanofilms with fs laser pulses has been shown to emit narrowband pulses with center frequencies ranging from 0.20 to 0.35 THz dependent on film composition[37], while theoretical models have explored acoustically-mediated spintronic emitters based on magneto-elastic heterostructures for converting fs laser pulses into ns-scale multi-cycle THz pulses[38]. A scheme combining an echelon, digital micro-mirror device and a spintronic emitter has demonstrated the generation of THz pulse trains[39] and photo-mixing has been used to produce a narrow-linewidth continuous-wave THz source[40]. These works highlight potential future opportunities in areas of on-chip THz emitters, THz magnonic devices and fast THz communication, yet key limitations in power, tunability and complexity of these narrowband THz generation schemes remain.

In this letter, we demonstrate that spintronic THz emitters can be driven with a simple chirped-pulse beating scheme to produce frequency- and bandwidth-tunable multi-cycle THz pulses. The simple optical setup, capability to scale to high fields through high-power laser amplifier systems and access to the unique properties of spintronic emitters make this an ideal source for narrowband applications over the entire THz spectral range.

Spintronic THz emitters exploit the interplay between ferromagnetic (FM) and non-magnetic (NM) thin films, using an ultrashort laser pulse to drive a spin-polarized current in the FM layer that is converted into a transverse charge current in the NM layer by the inverse spin-Hall effect. This ultrafast current generates single-cycle THz pulses polarized perpendicular to the magnetization of the FM layer, with a broadband spectrum only limited by the optical bandwidth of the drive laser.[2,3] The same ultrafast laser-induced dynamics can, however, be manipulated by temporal and spectral shaping of the drive laser to control the THz emission, which we demonstrate through the optical technique of chirped-pulse beating to generate narrowband THz pulses.

As first reported by Weling *et al.*[15], chirped-pulse beating involves the interferometric combination of two (or more) chirped laser pulses with a time delay (τ), resulting in an intensity modulation of the laser pulse profile at a frequency given by $f_{\text{beat}} = 2\ln(2)\tau/\pi\delta t_0\delta t_1$,[19] where δt_0 and δt_1 correspond to the FWHM duration of the transform-limited and chirped pulse intensities, respectively. This modulated laser pulse can be used to drive multi-cycle THz generation with a center frequency of $f_{\text{THz}} \approx f_{\text{beat}}$ over a range corresponding to the optical bandwidth of the laser pulse, with an intensity linewidth $\Delta f_{\text{THz}} \approx \Delta f = \ln(2)\sqrt{8}/\pi\delta t_1$,[19] providing narrowband THz pulses with simple frequency and bandwidth tuning controlled by the chirp and/or time delay.

To experimentally demonstrate chirped-pulse beating in a spintronic emitter, laser pulses from a commercial (Coherent, Legend) Ti:sapphire regenerative amplifier (1 mJ pulse energy, 1 kHz repetition rate, 800 nm central wavelength, 50 fs transform-limited pulse duration) were positively-chirped (6 ps or 12 ps FWHM) by detuning the compressor and routed to a home-made Gires-Tournois etalon consisting of a 38% partial reflector (PR) and ≈100% high-reflector (HR), as shown in Fig.1. The adjustable etalon gap, d, provided a tunable time delay of $\tau = 2d/c$ between laser pulses. The etalon produced a train of chirped pulses (with 38% of the laser energy in each of the first two pulses) as indicated in the inset of Fig.1, providing negligible power loss (all reflections contribute to THz generation) and improved interferometric stability compared to a standard Michelson interferometer. Due to the multiple reflections, the etalon-based scheme does result in the generation of THz harmonics,[22] which may not be desirable for certain applications.

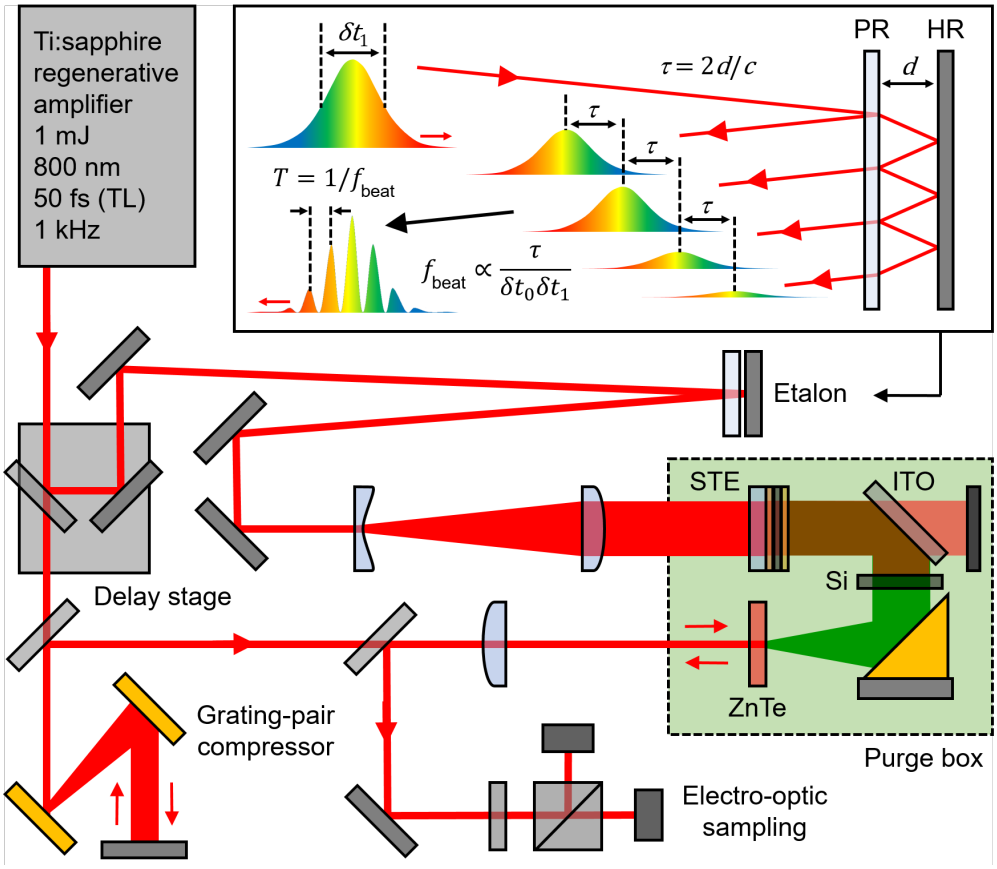

FIG. 1. Schematic diagram of the experimental setup for chirped-pulse beating in a spintronic THz emitter (STE). Inset: Concept of etalon-based chirped-pulse beating, using tunable separation d of the partial (PR) and high (HR) reflectors to control the time delay τ and corresponding beat frequency f_{beat} of the modulated laser pulse.

It should also be noted that while harmonic suppression due to phase-mismatch has been observed in organic crystal THz sources[18], this cannot be achieved in spintronic emitters as the generation process does not involve phase-matching.

The temporal intensity modulated laser pulse was used to generate multi-cycle THz pulses in a trilayer spintronic THz emitter, which were routed and focused by a 90 degree off-axis parabolic mirror with a 50.8 mm focal length onto a 500 μm-thick (110)-cut ZnTe crystal. Residual laser pump light transmitted through the spintronic emitter was blocked using a combination of an ITO-coated fused silica plate followed by a HRFZ-Si wafer. A probe laser pulse, separated off by transmission through a 90(R)/10(T) beamsplitter, was compressed back to its transform-limited 50 fs pulse duration with a grating-pair compressor and then used in a back-reflection geometry for THz pulse measurements in a standard electro-optic sampling scheme. The back-reflection

geometry is a convenient approach which allows greater control over the probe beam alignment independent of the THz focusing optics. For single-cycle THz measurements, the output of the regenerative amplifier laser was fully compressed and the etalon partial reflector was removed to excite the source with a single 50 fs pulse, while using the undiffracted zeroth-order from the probe grating compressor for detection.

The trilayer spintronic emitter had a nominal structure W (2 nm)/$Co_{20}Fe_{60}B_{20}$(2 nm)/Pt (2 nm) and was deposited onto a double-side polished 0.5 mm-thick fused silica substrate using DC-magnetron sputtering. The base pressure of the system was below $5x10^{-8}$ Torr and the Ar working gas was maintained at a pressure of 3 mTorr. No magnetic fields were applied during the deposition. Actual deposited layer thicknesses were determined using x-ray reflectivity (XRR) measurements, which are shown in the supplementary material. A saturating external magnetic field of 23 mT was applied in the plane of the film (vertically) to generate horizontally polarized THz pulses. Laser excitation with 0.7 mJ pulse energy and 20 mm ($1/e^2$) spot size provided a fluence of approximately 0.2 mJ/cm^2. All experiments were performed at room temperature in a dry-air purged environment with a relative humidity of approximately 10%.

The spintronic emitter was first characterized in the standard single-cycle configuration to aid optimization and analysis of the multi-cycle emission. This included extracting THz reflection features in the time domain, which were removed using a simple subtraction algorithm (see supplementary material on THz waveform reflection removal) to minimize distortions to the longer overlapping multi-cycle pulses. The reflection-corrected single-cycle waveform and corresponding broadband THz spectral intensity profile of the spintronic source are shown in Fig.2(a) and (b), with a bandwidth of approximately 3 THz. The electric field amplitude of the single-cycle emission was calculated, as described by Cliffe *et al.*,[41] to be 9 kV/cm. The chirped-pulse beating scheme was then implemented with laser pulses chirped to 6 ps FWHM (as measured by an intensity autocorrelator assuming a sech^2 pulse shape) with the generated multi-cycle THz waveforms and corresponding spectra shown in Fig.2(c) and (d). By tuning the etalon spacing ($d \approx 42$ - 232 μm), the equivalent time delays ($\tau = 0.28$ - 1.55 ps) resulted in center frequencies ranging from 0.4 to 2.3 THz, the approximate range over which our experimental configuration detected the single-cycle emission. In comparison to the single-cycle emission, the electric field amplitude of the multi-cycle emission was calculated to be 0.6 kV/cm at 0.7 THz, a value consistent with the factor of approximately 100 increase in the pump pulse duration, and the concurrent decrease in the pump intensity. The multi-peak structure appearing on the intensity spectra in Fig.2(d) as the

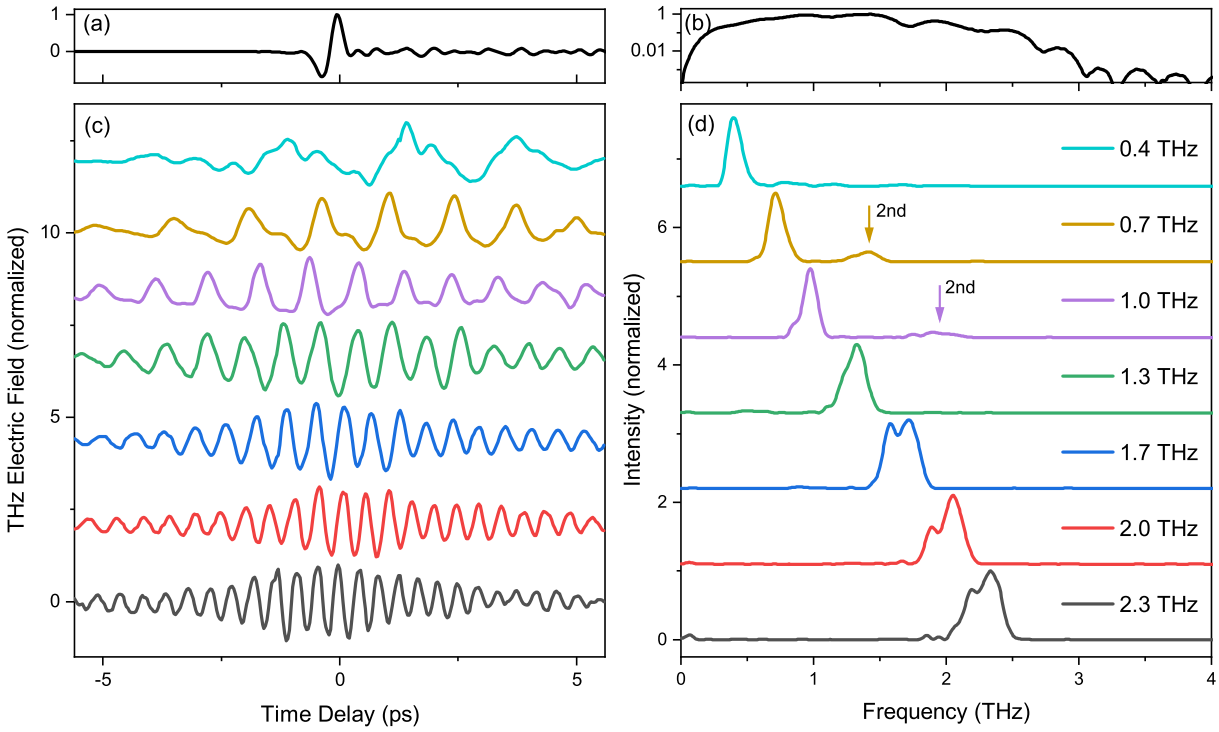

FIG. 2. (a) Single-cycle THz waveform emitted by the spintronic emitter when driven by a single transform-limited (50 fs) laser pulse and (b) corresponding intensity spectrum. (c) Multi-cycle THz waveforms generated by the chirped-pulse beating scheme using $\delta t_1 = 6$ ps for variable τ from 0.28 to 1.55 ps, with (d) the corresponding narrowband intensity spectra ranging from 0.4 to 2.3 THz. The THz waveforms and intensity spectra are normalized and vertically offset for clarity (see supplementary material on THz spectra for un-normalized intensity spectra). The arrows indicate the position of the second harmonic peaks.

frequency increases is a Fourier-transform artifact resulting from a non-complete removal of the substrate/air reflection in the THz waveform at 6.7 ps (see supplementary material on reflection removal).

As expected, and observed previously by Chen et al.[22] using a $LiNbO_3$ THz source, an etalon-based chirped-pulse beating scheme generates THz harmonics, see Fig.2(d). These features are evident for the lower fundamental frequencies (for example at 0.7 THz and 1.0 THz) where the second harmonics (1.4 THz and 2.0 THz) reside within the THz frequency range afforded by the response function of the ZnTe detection crystal and the optical bandwidth of the laser pulse. In addition, Δf_{THz} is observed to increase with f_{THz}, from 128 GHz at 0.4 THz to 287 GHz at 2.3 THz, as shown in Fig.3. This spectral broadening was attributed to higher-order phase modulation[15] inherent to chirped-pulse amplification (CPA)-based laser systems, where third-order dispersion

adds curvature to the chirp that results in varying f_{beat} along the duration of the chirped pulse beating output.

To verify our experimental results and develop a greater understanding of the multi-cycle THz generation process in a spintronic emitter, we considered the dynamics of the generated spin-polarized current. The microscopic 3-temperature model (M3TM)[42,43] is commonly used to determine the temporal dynamics of laser demagnetization, which in turn has been shown to share identical physical processes with laser-induced spin current generation[44–47], since the generated spin current is proportional to the rate of change of the magnetization. The M3TM describes the temperature dependence of the electrons and phonons, and through a series of differential equations that couple with each other, the temporal evolution of the magnetization.

As detailed in the supplementary material, our M3TM calculations used a CoFeB/Pt bilayer source instead of a W/CoFeB/Pt trilayer to simplify the calculation, with parameter values summarized in Table S2. The model provided the temperature variation of electrons T_{e} and phonons T_{ph} in the CoFeB and Pt layers after laser excitation, and the resulting laser-induced demagnetization in the CoFeB layer. Consequently, the temporal profile and spectrum of the spin current j_s were obtained from the temporal derivative of the magnetization of the CoFeB layer. For our chirped-pulse-beating scheme, the temporally modulated laser pulse drove corresponding modulation of the T_{e} and T_{ph} dynamics, and ultimately the demagnetization, forming a multi-cycle spin current that led to generation of multi-cycle THz pulses.

The inset of Fig.3 shows the output from our model calculations, verifying the narrowband THz emission is accompanied by an increase in Δf_{THz} with f_{THz}. It should be noted that, using the approach of Weling *et al.*[15], the expression for the chirped-pulse beating intensity modulation was modified to include an additional chirp modulation term, $3\alpha\tau t^2$, where the cubic phase coefficient, α, was fixed at a value of $\alpha = 0.045\,\text{rad/ps}^3$ in order to account for the quadratic chirp of our laser pulses (inherent to CPA-based laser systems, as highlighted in the discussion of the experimental data and by Jolly *et al.*[48]), and reproduce the experimental data in Fig.2(d). The cubic phase coefficient, α, can be used to calculate the frequency sweep rate of the resulting linearly-chirped THz pulses (given by $6\alpha\tau/2\pi$), giving values ranging from 12×10^{21} to 67×10^{21} Hz/sec which are consistent with values reported in the literature when using a grating-based pulse stretcher.[49] A comparison of Δf_{THz} from both experiment and model is shown in Fig.3, and demonstrates good correlation, although some experimental linewidth values are clearly distorted by the Fourier-transform oscillation artifact (discussed earlier). Without the inclusion of the chirp modulation

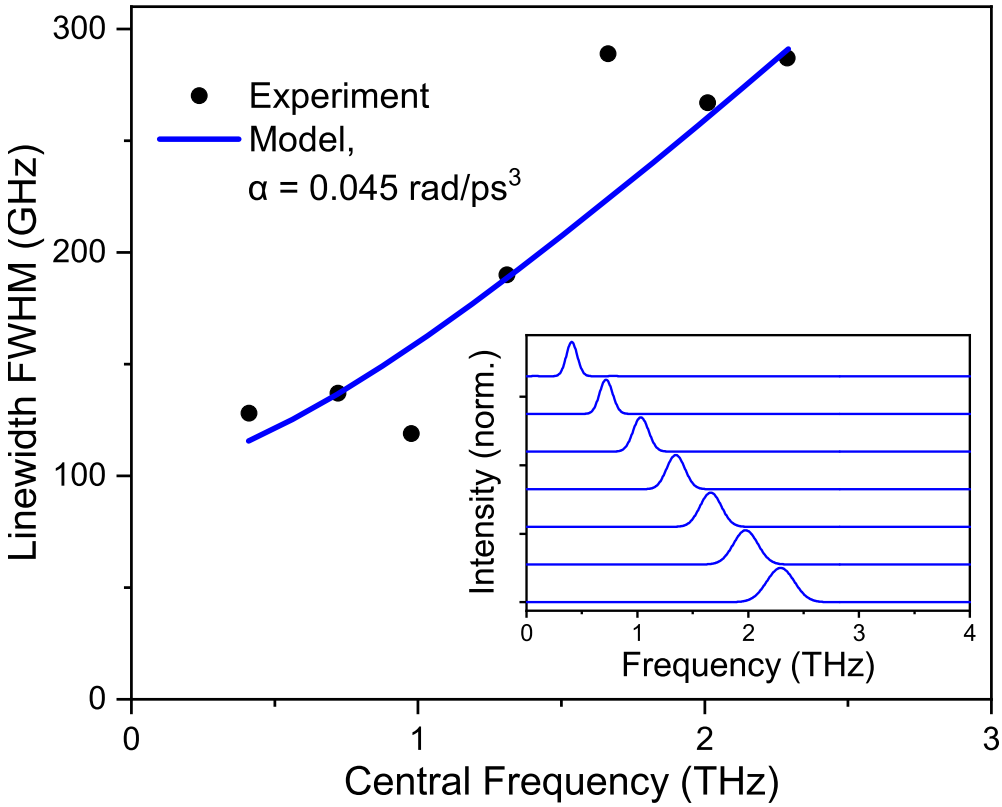

FIG. 3. Linewidth of the THz intensity spectra in Fig.2 (d) as a function of the THz center frequency. The blue line is the result of a model calculation described in the main text (and supplementary material), where the cubic phase coefficient α has a value of $0.045\,\mathrm{rad/ps^3}$. Inset: The intensity spectra from the model calculations.

term Δf_{THz} was constant at 107 GHz.

While spectral broadening due to cubic phase modulation can be suppressed by modifying the relative spectral phase of the chirped pulses,[48] or eliminated by using a second grating pair,[50] we simply demonstrate the capability for narrower linewidth emission from a spintronic THz emitter by chirping the laser pulse to approximately 12 ps and tuning the emission to 0.4 THz (where the contribution from the cubic phase modulation is reduced). The resulting THz intensity spectrum is shown in Fig.4 and the corresponding waveform in the inset. At a center frequency of $f_{\mathrm{THz}} = 0.4$ THz (with the second harmonic observed at 0.8 THz), a linewidth of $\Delta f_{\mathrm{THz}} = 41$ GHz was achieved. The linewidth is consistent with the values reported by Adamonis *et al.*[17] using a photoconductive antenna, where linewidths of 50-65 GHz over the frequency range 0.19-1 THz were achieved with a laser pulse that was chirped to 15 ps.

In conclusion, we demonstrate that spintronic THz emitters can be driven with a simple

chirped-pulse beating scheme to produce frequency- and bandwidth-tunable multi-cycle THz pulses. Model calculations reveal that this is possible as the intensity modulation generated from the interferometric combination of two chirped pulses can be converted into a modulation of the spin-polarized current due to the rapid demagnetization of the ferromagnetic film[42]. Given the gap-free ultra-broadband nature of spintronic THz emission shown previously with ultrashort 10 fs drive pulses, and that 10 fs pulses can be chirped to nearly 1 ns,[51] our proof-of-concept results pave the way towards a narrowband THz source with sub-GHz linewidth and center frequency continuously tunable over the entire THz spectral range from 0.1 to 30 THz.

The supplementary material contains details of the x-ray reflectivity measurements, reflection removal from the THz waveforms, and the model calculations describing the multi-cycle THz generation mechanism in the spintronic emitter.

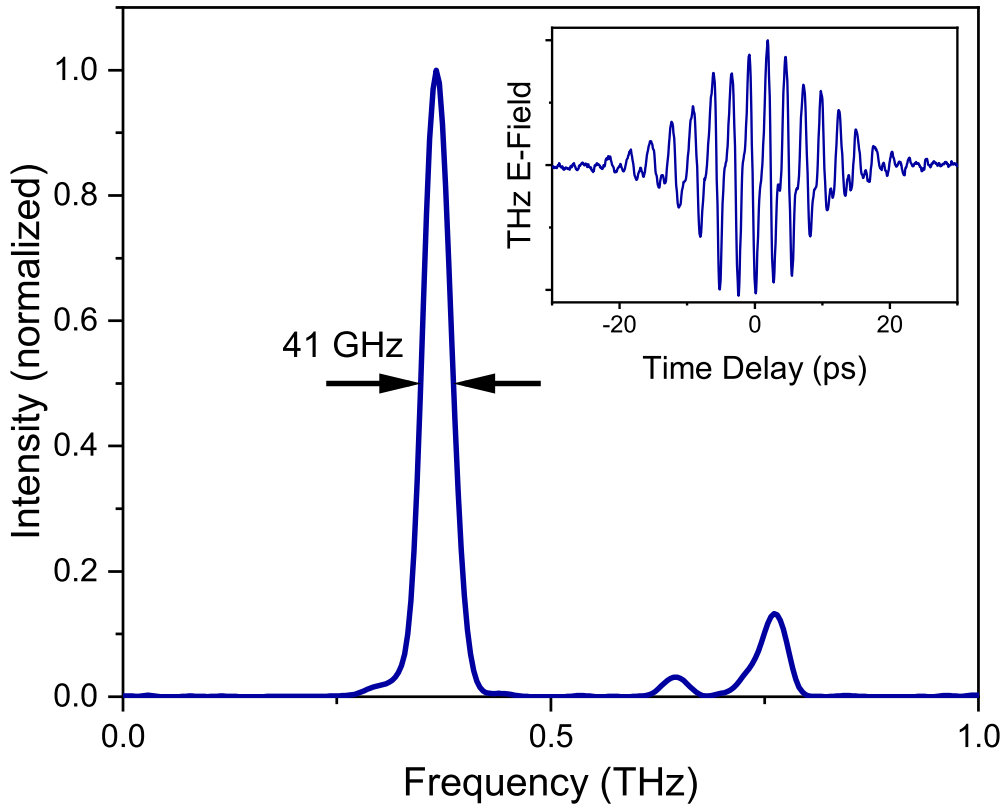

FIG. 4. The measured narrowband THz intensity spectrum for chirped-pulse beating in the spintronic THz emitter using a chirped laser pulse duration of approximately 12 ps. Inset: Corresponding THz waveform.

This work was supported by the United Kingdom Engineering and Physical Sciences Research Council [Grant No. EP/S033688/1]. We also wish to acknowledge the Ph.D. scholarship support for R. Ji by the China Scholarship Council (NSCIS Grant No. 201906120039).

DATA AVAILABILITY

The data associated with the paper are openly available from the Zenodo data repository at: http://dx.doi.org/xx.xxxxx/xxxxxxxxxxxx.

REFERENCES

[1]E. Beaurepaire, J.-C. Merle, A. Daunois, and J.-Y. Bigot, Phys. Rev. Lett. **76**, 4250 (1996).

[2]T. Kampfrath, M. Battiato, P. Maldonado, G. Eilers, J. Nötzold, S. Mährlein, V. Zbarsky, F. Freimuth, Y. Mokrousov, S. Blügel, M. Wolf, I. Radu, P. M. Oppeneer, and M. Münzenberg, Nat. Nanotechnol. **8**, 256 (2013).

[3]C. Bull, S. M. Hewett, R. Ji, C.-H. Lin, T. Thomson, D. M. Graham, and P. W. Nutter, APL Mater. **9**, 090701 (2021).

[4]R. Rouzegar, A. L. Chekhov, Y. Behovits, B. R. Serrano, M. A. Syskaki, C. H. Lambert, D. Engel, U. Martens, M. Münzenberg, M. Wolf, G. Jakob, M. Kläui, T.S. Seifert, and T. Kampfrath, Phys. Rev. Appl. **19**, 034018 (2023).

[5]T. Seifert, S. Jaiswal, U. Martens, J. Hannegan, L. Braun, P. Maldonado, F. Freimuth, A. Kronenberg, J. Henrizi, I. Radu, E. Beaurepaire, Y. Mokrousov, P. M. Oppeneer, M. Jourdan, G. Jakob, D. Turchinovich, L. M. Hayden, M. Wolf, M. Münzenberg, M. Kläui, and T. Kampfrath, Nat. Photonics **10**, 483 (2016).

[6]T. Seifert, S. Jaiswal, M. Sajadi, G. Jakob, S. Winnerl, M. Wolf, M. Kläui, and T. Kampfrath, Appl. Phys. Lett. **110**, 252402 (2017).

[7]M. T. Hibberd, D. S. Lake, N. A. B. Johansson, T. Thomson, S. P. Jamison, and D. M. Graham, Appl. Phys. Lett. **114**, 031101 (2019).

[8]D. Kong, X. Wu, B. Wang, T. Nie, M. Xiao, C. Pandey, Y. Gao, L. Wen, W. Zhao, C. Ruan, J. Miao, Y. Li, L. Wang Adv. Opt. Mater. **7**, 1900487 (2019).

[9]S. M. Hewett, C. Bull, A. M. Shorrock, C.-H. Lin, R. Ji, M. T. Hibberd, T. Thomson, P. W. Nutter, and D. M. Graham, Appl. Phys. Lett. **120**, 122401 (2022).

[10]A. Dienst, E. Casandruc, D. Fausti, L. Zhang, M. Eckstein, M. Hoffmann, V. Khanna, N. Dean, M. Gensch, S. Winnerl, W. Seidel, S. Pyon, T. Takayama, H. Takagi and A. Cavalleri, Nat. Mater. 12, 535 (2013).

[11]K. Uchida, H. Hirori, T. Aoki, C. Wolpert, T. Tamaya, K. Tanaka, T. Mochizuki, C. Kim, M. Yoshita, H. Akiyama, L. N. Pfeiffer, and K. W. West, Appl. Phys. Lett. **107**, 221106 (2015).

[12]K. Brekhov, V. Bilyk, A. Ovchinnikov, O. Chefonov, V. Mukhortov, and E. Mishina, Nanomaterials **13**, 1961 (2023).

[13]T. Lin, R. Xu, X. Chen, Y. Guan, M. Yao, J. Zhang, X. Li, and H. Zhu, Optica Open. Preprint. (2023) https://doi.org/10.1364/opticaopen.22066295.v2

[14]M. T. Hibberd, A. L. Healy, D. S. Lake, V. Georgiadis, E. J. H. Smith, O. J. Finlay, Thomas H. Pacey, James K. Jones, Yuri Saveliev, D. A. Walsh, E. W. Snedden, R. B. Appleby, G. Burt, D. M. Graham and S. P. Jamison, Nat. Photonics **14**, 755 (2020).

[15]A. S. Weling and D. H. Auston, J. Opt. Soc. Am. B **13**, 2783 (1996).

[16]J. Krause, M. Wagner, S. Winnerl, M. Helm, and D. Stehr, Opt. Express **19**, 19114 (2011).

[17]J. Adamonis, N. Rusteika, R. Danilevičius, and A. Krotkus, Opt. Commun. **293**, 61 (2013).

[18]J. Lu, H. Y. Hwang, X. Li, S.-H. Lee, O-P. Kwon, and K. A. Nelson, Opt. Express **23**, 22723 (2015).

[19]A. V. Ovchinnikov, O. V. Chefonov, M. B. Agranat, V. E. Fortov, M. Jazbinsek, and C. P. Hauri, Opt. Express **28**, 33921 (2020).

[20]C. Vicario, A. Trisorio, S. Allenspach, C. Rüegg, and F. Giorgianni, Appl. Phys. Lett. **117**, 101101 (2020).

[21]J. R. Danielson, A. D. Jameson, J. L. Tomaino, H. Hui, J. D. Wetzel, Yun-Shik Lee, and K. L. Vodopyanov, J. Appl. Phys. **104**, 033111 (2008).

[22]Z. Chen, X. Zhou, C. A. Werley, and K. A. Nelson, Appl. Phys. Lett. **99**, 071102 (2011).

[23]X. Zhou, Y. Lin, Y. Chan, F. Deng, and J. Zhang, Opt. Lett. 48, 2881 (2023).

[24]A. Sell, A. Leitenstorfer, and R. Huber, Opt. Lett. **33**, 2767 (2008).

[25]B. Liu, H. Bromberger, A. Cartella, T. Gebert, M. Först, and A. Cavalleri, Opt. Lett. **42**, 129-131 (2017).

[26]K. L. Vodopyanov; M. M. Fejer; X. Yu; J. S. Harris; Y.-S. Lee; W. C. Hurlbut; V. G. Kozlov; D. Bliss; C. Lynch, Appl. Phys. Lett. **89**, 141119 (2006)

[27]I. Tomita, H. Suzuki, H. Ito, H. Takenouchi, K. Ajito, R. Rungsawang, and Y. Ueno, Appl. Phys. Lett. **88**, 071118 (2006)

[28]C. Zhang, Y. Avetisyan, A. Glosser, I. Kawayama, H. Murakami, M. Tonouchi, Opt. Express **20**, 8784 (2012).

[29]F. Lemery, T. Vinatier, F. Mayet, R. Aßmann, E. Baynard, J. Demailly, U. Dorda, B. Lucas, A.-K. Pandey, and M. Pittman, Commun. Phys. **3**, 150 (2020).

[30]C. D. W. Mosley, D. S. Lake, D. M. Graham, S. P. Jamison, R. B. Appleby, G. Burt, M. T. Hibberd, Opt. Express **31**, 4041 (2023).

[31]W. Tian, G. Cirmi, H. T. Olgun, P. Mutter, C. Canalias, A. Zukauskas, L. Wang, E. Kueny, F. Ahr, A.-L. Calendron, F. Reichert, K. Hasse, Y. Hua, D. N. Schimpf, H. Çankaya, M. Pergament, M. Hemmer, N. Matlis, V. Pasiskevicius, F. Laurell, F. X Kärtner, Opt. Lett. **46**, 741 (2021).

[32]T. J. Edwards, D. Walsh, M. B. Spurr, C. F. Rae, M. H. Dunn, and P. G. Browne, Opt. Express **14**, 1582 (2006).

[33]D. J. M. Stothard, T. J. Edwards, D. Walsh, C. L. Thomson, C. F. Rae, M. H. Dunn, and P. G. Browne, Appl. Phys. Lett. 92, 141105 (2008).

[34]D. Walsh, D. J. M. Stothard, T. J. Edwards, P. G. Browne, C. F. Rae, and M. H. Dunn, J. Opt. Soc. Am. B **26**, 1196 (2009).

[35]D. Jang, K.-Y. Kim, Opt. Express **28**, 21220 (2020).

[36]B. Zhang, X. Wu, X. Wang, S. Li, J. Ma, G. Liao, Y. Li, and J. Zhang, Opt. Lett. **47**, 2678 (2022).

[37]N. Awari, S. Kovalev, C. Fowley, K. Rode, R. A. Gallardo, Y.-C. Lau, D. Betto, N. Thiyagarajah, B. Green, O. Yildirim, J. Lindner, J. Fassbender, J. M. D. Coey, A. M. Deac, and M. Gensch, Appl. Phys. Lett. **109**, 032403 (2016).

[38]S. Zhuang, P. B. Meisenheimer, J. Heron, and J.-M. Hu, ACS Appl. Mater. Interfaces **13**, 48997 (2021).

[39]J. E. Nkeck, L.-P. Béliveau; X. Ropagnol, D. Deslandes, D. Morris, and F. Blanchard, APL Photonics **7**, 126105 (2022).

[40]P. Kolejak, G. Lezier, S. Kassi, L. Dhevarhidjian, M.-A. Martin, O. Pirali, G. Ducournau, J.-F. Lampin, N. Tiercelin, and M. Vanwolleghem, 47th International Conference on Infrared, Millimeter and Terahertz Waves (IRMMW-THz), Delft, Netherlands, (2022), pp. 1-2, doi: 10.1109/IRMMW-THz50927.2022.9896051.

[41]M. J. Cliffe, D. M. Graham, and S. P. Jamison, Appl. Phys. Lett. **108**, 221102 (2016).

[42]B. Koopmans, G. Malinowski, F. Dalla Longa, D. Steiauf, M. Fähnle, T. Roth, M. Cinchetti, and M. Aeschlimann, Nat. Mater. **9**, 259 (2010).

[43]K. Kuiper, T. Roth, A. Schellekens, O. Schmitt, B. Koopmans, M. Cinchetti, and M. Aeschlimann, Appl. Phys. Lett. **105**, 202402 (2014).

[44]M. Beens, R. A. Duine, and B. Koopmans, Phys. Rev. B. **105**, 144420 (2022).

[45]G.-M. Choi, B.-C. Min, and K.-J. Lee, and D. G. Cahill, Nat. Commun. **5**, 4334 (2014).

[46]J. Kimling and D. G. Cahill, Phys. Rev. B. **95**, 014402 (2017).

[47]R. Rouzegar, L. Brandt, L. Nádvorník, D. A. Reiss, A. L. Chekhov, O. Gueckstock, C. In, M. Wolf, T. S. Seifert, P. W. Brouwer, G. Woltersdorf, and T. Kampfrath, Phys. Rev. B. **106**, 144427 (2022).

[48]S. W. Jolly, N. H. Matlis, F. Ahr, V. Leroux, T. Eichner, A.-L. Calendron, H. Ishizuki, T. Taira, F. X. Kärtner, and A. R. Maier, Nat. Commun. **10**, 2591 (2019).

[49]S. Kamada, T. Yoshida, and T. Aoki, Appl. Phys. Lett. **104**, 101102 (2014).

[50]T. Yoshida, S. Kamada, and T. Aoki, Opt. Express 22, 23679 (2014).

[51]C. P. J. Barty, T. Guo, C. Le Blanc, F. Raksi, C. Rose-Petruck, J. Squier, K. R. Wilson, V. V. Yakovlev, and K. Yamakawa, Opt. Lett. **21**, 668 (1996).